NAR Cancer, 2025, **7**, zcaf017
https://doi.org/10.1093/narcan/zcaf017
Cancer Gene Regulation, Chromatin, and Epigenetics

Leveraging the interconnected unfolded protein response and NLRP3 inflammasome pathways to reactivate Epstein–Barr virus in diffuse large B-cell lymphomas

Huanzhou Xu [1], Tarun E. Hutchinson [2], Siva Koganti [1], Beth A. Rousseau [1], Daniel Xia [2], Michael T. McIntosh [2,3], Sumita Bhaduri-McIntosh [1,3,*]

[1]Division of Infectious Diseases, Department of Pediatrics, University of Florida, Gainesville, FL 32610, United States
[2]Child Health Research Institute, Department of Pediatrics, University of Florida, Gainesville, FL 32610, United States
[3]Department of Molecular Genetics and Microbiology, University of Florida, Gainesville, FL 32610, United States
[*]To whom correspondence should be addressed. Email: sbhadurimcintosh@ufl.edu

Abstract

Diffuse large B-cell lymphoma (DLBCL), when associated with Epstein–Barr virus (EBV) in immunocompromised individuals such as AIDS patients, presents a significant treatment challenge. Lytic induction therapy, which reactivates latent EBV to directly kill tumor cells and sensitize them to nucleoside analogs that block viral replication and immune clearance, offers promise. However, little is known about EBV reactivation in DLBCL. Here, we examined four EBV-positive DLBCL cell lines and found variable, cell-line-specific responses to lytic stimuli, with most showing an abortive response—either before or after genome replication, without virus release. This is in contrast to commonly studied lymphoma cells in which EBV reactivation typically leads to a full lytic cycle. Mechanistically, we show that the unfolded protein response (UPR), via a splice variant of the transcription factor XBP1, upregulates TXNIP and NLRP3, activating the inflammasome and removing a barrier to transcription of the EBV latent-to-lytic switch gene *BZLF1*. Combining lytic induction with the nucleoside analog ganciclovir enhanced oncolytic cell death. This study identifies a pivotal link between two danger sensing pathways, the UPR and the inflammasome, in reactivating the virus resident in DLBCL and suggests that controlled lytic reactivation could provide a basis for EBV-targeted therapies to improve outcomes in this malignancy.

Graphical abstract

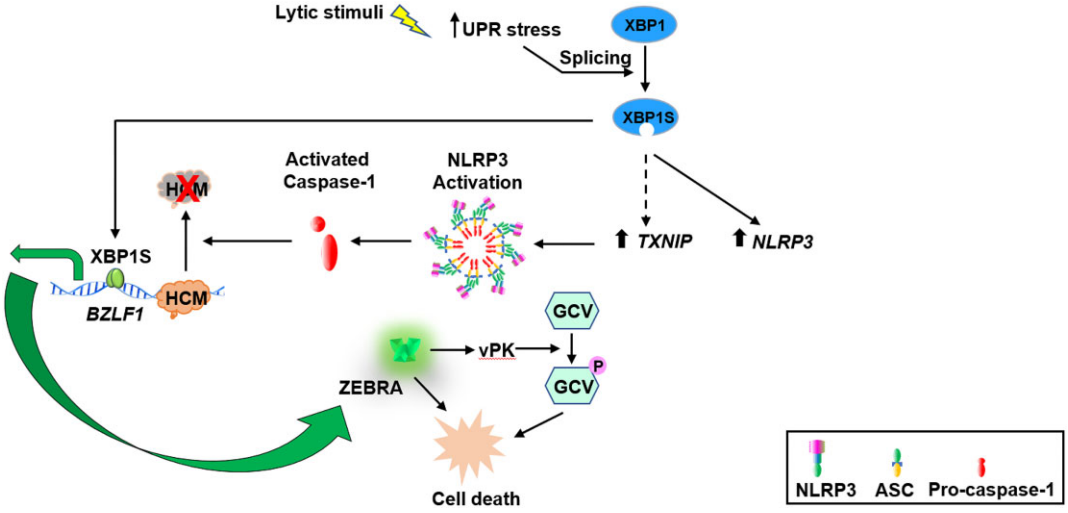

Introduction

Diffuse large B-cell lymphoma (DLBCL) is the most prevalent form of non-Hodgkin lymphoma and is known for its aggressive nature. Despite the use of advanced therapies that include rituximab or anti-CD20 monoclonal antibody alongside chemotherapy with cyclophosphamide, hydroxydaunorubicin/doxorubicin, oncovin/vincristine, and prednisone (R-CHOP), nearly 50% of patients either experience refractory disease or relapse [1]. The presence of Epstein–Barr virus (EBV), classified by the WHO as a class I carcinogen,

Received: December 10, 2024. **Revised:** March 31, 2025. **Editorial Decision:** April 16, 2025. **Accepted:** April 25, 2025

further complicates DLBCL prognosis [2, 3]. EBV-positive DLBCL, not otherwise specified (NOS), accounts for up to 15% of DLBCL cases in non-HIV patients but a significantly higher 30%–90% in AIDS patients [4–6]. Consequently, patients with AIDS-related EBV$^+$ DLBCL face particularly challenging outcomes despite improvements in chemotherapy and antiretroviral therapy [7, 8].

To improve outcomes for DLCBL, novel therapeutic strategies should target the biology of EBV, a herpesvirus. One promising approach causes death of EBV$^+$ lymphomas through oncolysis wherein latent EBV in the tumor cell is forced into the lytic/replicative state. Supporting this strategy, a phase 1b/2 clinical trial shows promise in treating EBV$^+$ lymphomas, including DLBCL resistant to R-CHOP [9]. However, successful application of this approach will require identifying the specific triggers that reactivate EBV in DLBCL and understanding the mechanisms of the latent-to-lytic transition in these tumors.

EBV has been extensively studied in cell lines derived from explanted Burkitt lymphomas (BL) and lymphoblastoid cell lines (B lymphocytes transformed *in vitro* by EBV, aka LCL). EBV initially infects epithelial and B cells through saliva. In B lymphocytes, the virus assumes a latent/silent state to persist in over 95% of the human population. Reactivation into the lytic phase, triggered by as-yet-unclear *in vivo* factors, occurs in a subset of latently infected B cells. This reactivation requires the expression of the EBV immediate-early lytic gene product, ZEBRA, a transcription and replication factor encoded by the viral ORF *BZLF1*, which is not expressed during latency. The expression of ZEBRA initiates a cascade of events including transcriptional activation of early lytic genes, many of which encode components of the viral genome replication machinery. Early gene expression is followed by replication of the viral genome, transcription of late lytic genes (that encode structural components of the virus) from newly replicated EBV genomes, packaging of new EBV genomes, and the assembly and release of infectious viral particles. These particles can then infect new cells within the host or spread to others [10].

While there is some understanding of the various latency profiles of EBV in DLBCL and the identity of latency-related viral oncogene expression, knowledge about the lytic phase is limited to detection of a few EBV lytic proteins in a small fraction of cells within primary DLBCL [11, 12]. Several important questions remain unanswered: Can EBV be experimentally and potentially therapeutically switched into the lytic phase? Are DLBCL-derived tumor lines responsive to known lytic triggers? What proportion of cells in DLBCL lines can support EBV's transition to the lytic phase? What cellular mechanisms drive the activation of ZEBRA in DLBCL? Does the lytic phase in DLBCL cells proceed to completion, including viral genome replication, packaging, and the release of virus particles? Can lytic reactivation effectively kill DLBCL cells? Answering these questions is essential for developing strategies to oncolytically target and eliminate EBV-positive DLBCL.

To answer these questions, it is essential to establish a foundational understanding of the EBV lytic phase in cell lines derived from EBV$^+$ DLBCL. We therefore examined four readily available EBV$^+$ DLBCL lines: two from HIV-negative individuals and two from AIDS patients. These cells exhibited minimal to no spontaneous lytic activity under baseline conditions. However, when exposed to five different lytic cycle triggers—each from a distinct chemical class and known to act through various pathways—the cells displayed varying levels of lytic response. Mechanistically, the DLBCL cells upregulated a cytoplasmic splice variant of XBP1, typically associated with the unfolded protein response (UPR). The splice variant, XBP1S, a transcription factor, increased the abundance of transcripts and proteins of the NLR family pyrin domain containing protein 3 (NLRP3) and thioredoxin-interacting protein (TXNIP), leading to inflammasome activation, which is a key upstream mechanism for EBV lytic reactivation [13, 14]. In effect, two innate immune platforms, the UPR and the inflammasome, collaborate to initiate EBV lytic activation in DLBCL cells. Remarkably, while one innate arm, the inflammasome, is known to remove barriers to reactivation, the other, the UPR, also provides a positive drive for reactivation via spliced XBP1-mediation transcription of *BZLF1*. Of medical interest, once the virus reactivated, the lytic phase tended to be abortive as the viral genome frequently did not replicate—but if it did, the DLBCLs demonstrated enhanced susceptibility to oncolytic killing by the nucleoside analog ganciclovir.

Materials and methods

Cell lines and chemical agents

EBV-positive VAL and EBV-negative SUDHL6 (kind gifts from Dr Izidore Lossos, University of Miami) and EBV-positive Farage (a kind gift from Dr Eric C. Johannsen, University of Wisconsin) cells were maintained in RPMI 1640 medium supplemented with 10% fetal bovine serum and 1% penicillin/streptomycin. EBV-positive IBL-1 and BCKN-1 cells (kind gifts from Dr Ethel Cesarman, Weill Cornell Medical College) were maintained in RPMI 1640 medium supplemented with 20% fetal bovine serum and 1% penicillin/streptomycin. All cell lines were cultured in a 37°C incubator with 5% CO_2.

For chemical treatment, 5×10^5/ml VAL, Farage and IBL-1, or 1×10^5/ml BCKN-1 cells were seeded with fresh medium and 24 h later, cells were spun down and re-suspended with fresh medium at 5×10^5/ml and incubated with 3 mM NaB (303 410, Sigma–Aldrich), 5 μM AZA (189826, Sigma–Aldrich), 200 μg/ml AffiniPure™ F(ab′)$_2$ fragment goat anti-Human IgG (H + L) (109-006-003, Jackson ImmunoResearch), 20 ng/ml of 12-O-Tetradecanoylphorbol-13-Acetate (TPA, 4174, Cell Signaling), 20 ng/ml of transforming growth factor beta (TGF-β, 11409-BH-010, R&D systems), NaB + TPA (3 mM + 20 ng/ml) or NaB + TGF-β (3 mM + 20 ng/ml) for 24 or 48 h. To induce UPR/endoplasmic reticulum (ER) stress, cells were pre-incubated with different concentrations of tunicamycin (TM; T7765, Sigma–Aldrich) for 2 h followed by induction with 3 mM NaB for another 24 h. To inhibit ER stress, cells were pre-incubated with different concentrations of 4μ8C (SML0949, Sigma–Aldrich) for 2 h followed by induction with 3 mM NaB for another 24 h. To inhibit the NLRP3 inflammasome, VAL cells were treated with 5 μM MCC950 (538120, Sigma–Aldrich) for 6 h followed by induction with lytic stimuli for another 24 or 48 h.

Immunoblotting and antibodies

Immunoblotting was conducted as described previously [15]. Briefly, cells were lysed using radioimmunoprecipitation assay (RIPA) buffer and subjected to electrophoresis on

10% sodium dodecyl sulfate-polyacrylamide gels. Following separation, immunostaining was performed with the specified antibodies. The following antibodies were used: mouse anti-ZEBRA BZ1 antibody (generously provided by Paul Farrell, Imperial College London), mouse anti-β-actin antibody (AC-15, Sigma–Aldrich), rabbit anti-NLRP3 antibody (19771-1, Proteintech), rabbit anti-TXNIP antibody (14715, Cell Signaling Technology), rabbit anti-Caspase 1 (Cleaved Asp210) antibody (PA538099, Thermo Fisher Scientific), rabbit anti-Caspase 1 antibody (PA587536, Thermo Fisher Scientific), rabbit anti-XBP1S antibody (24868, Proteintech), horseradish peroxidase (HRP)-conjugated goat anti-mouse IgG (626520, Thermo Fisher Scientific), and HRP-conjugated goat anti-rabbit IgG (31460, Thermo Fisher Scientific).

Flow cytometry

To measure the frequency of lytic cells, lytic trigger-exposed cells were stained as previously described [16]. Briefly, 24 or 48 h after exposure to inducers, the cells were fixed and permeabilized following an established protocol. Cells were then incubated with mouse anti-ZEBRA BZ1 antibody or mouse IgG (557273, BD Biosciences) as isotype control followed by incubation with goat anti-mouse conjugated to FITC (F0257, Sigma). Gates were drawn by comparing to cells stained with the isotype control antibody.

small interfering RNAs (siRNAs) and transfection

Transfection was performed as described previously [17]. Briefly, cells were maintained in fresh medium for 24 h. Then, one million cells were transfected with 200 pmol siRNA in transfection solution (MIR50117, Mirus) using an Amaxa Nucleofector II and the O-006 program. siRNAs used in this study included those targeting *NLRP3* (#1, s41554; #2, s41555, Thermo Fisher Scientific), *TXNIP* (#1, s20878; #2, s20879, Thermo Fisher Scientific), *XBP1*(#1, 5356; #2, 5533, Thermo Fisher Scientific). For XBP1S overexpression, 20 μg of pCMV5-Flag-XBP1s (63680, Addgene) [18] were transfected into one million cells.

Quantitative reverse transcriptase polymerase chain reaction

Quantitative reverse transcriptase polymerase chain reaction (RT-qPCR) was carried out as previously described [17]. Briefly, cDNA was synthesized using 1 μg of RNA and MuLV Reverse Transcriptase (M0253L, New England Biolabs). Quantitative PCR (qPCR) data were analyzed by normalizing to 18S rRNA using the ΔΔCT method. The primers used for RT-qPCR analysis are as follows. 5′GTAACCCGTTGAACCCCATT3' (forward) and 5′CCATCCAATCGGTAGTAGCG3' (reverse) for 18S rRNA; 5′GACCCATACCAGGTGCCTTTTG3' (forward) and 5′GCACACAAGGCAAAGGAGCTTG3' (reverse) for *BZLF1*; 5′CGGTTTGAGCACCCTCATCT3' (forward) and 5′GGCAAACGTGTAGGAGGTCA3' (reverse) for *BGLF4*; 5′ TGCACACCGTGGTGTTCCAG3' (forward) and 5′ GGCTCACCTCCCGACAGTG3' (reverse) for *NLRP3*; 5′ AGTTCGGCTTTGAGCTTCCTC3' (forward) and 5′ TTGAGTTGGCTGGCTCGGG3' (reverse) for *TXNIP*; 5′ CGTTCCGGAGCTGGGTATCTC3' (forward) and 5′CACCAAGCAGAGAGGACATGT3' (reverse) for *XBP1*.

qPCR to quantitate EBV load

Cell-associated EBV DNA was extracted as described earlier [19], and relative viral DNA levels were quantified through qPCR by targeting the EBV *BALF5* gene. To measure the relative amount of released EBV particles, equal volumes of culture supernatants were treated with DNase, and then qPCR was performed using primers specific to the EBV *BALF5* gene. The primers used to amplify EBV *BALF5* gene are as follows. 5′CGTCTCATTCCCAAGTGTTTC3′ (forward) and 5′GCCCTTTCCATCCTCGTC3′ (reverse).

Cell proliferation assay

Proliferation assays were performed as described previously [15]. Briefly, 2×10^5 VAL, IBL-1 and SUDHL6 DLBCLs were seeded in 24-well cell culture plates containing the indicated EBV lytic inducers with or without 40 μM ganciclovir (GCV). DMSO or GCV alone was set as control. Cells were spun down and resuspended in fresh medium containing GCV every 48 h. After 168 h (VAL and SUDHL6) or 96 h (IBL-1), cells were collected and subjected to propidium iodide (PI) (Sigma–Aldrich #P4864) staining and analyzed by flow cytometry to determine the numbers of live cells.

Statistical analysis

Student's *t*-test was used to assess statistical significance when performing pair-wise comparisons. Results are expressed as the mean ± standard error of the mean (SEM) for replicate experiments as indicated. *P*-values were calculated using Microsoft Excel or GraphPad Prism5. The degree of significance was indicated as $*P < 0.05$; $**P < 0.01$; $***P < 0.001$.

Results

EBV⁺ DLBCLs display variable responsiveness to agents that induce the EBV lytic cycle

Forcing EBV's transition into the lytic phase is a strategy to directly lyse tumor cells producing virus particles, abort progress of the lytic phase by ensuring incorporation of toxic nucleoside analogs into the viral genome, and activate the immune response to clear tumor cells. Common lytic phase inducers include sodium butyrate (NaB) and azacytidine (AZA), both acting as epigenetic modifiers that trigger lytic gene expression [20]. TPA, a phorbol ester, triggers protein kinase C (PKC) to initiate the lytic cycle [21], TGF-β utilizes AP-1 and Smad proteins to facilitate EBV reactivation [22, 23], and IgG can mimic immune triggers of lytic reactivation [24]. Furthermore, combination treatments with NaB plus TPA or TGF-β have shown enhanced reactivation by utilizing synergistic mechanisms [20].

To investigate response to lytic triggers, VAL, IBL-1, Farage, and BCKN-1 DLBCL cells were exposed to lytic cycle inducing agents NaB, AZA, IgG, TGF-β, and combinations for different durations. Flow cytometric analysis of ZEBRA⁺ cells revealed variable induction of the EBV lytic phase across different cell lines (Figs 1A, 2A, 3A, and 4A). In VAL cells, we observed some spontaneous lytic reactivation with 2.9% uninduced cells expressing ZEBRA at baseline. Exposure to all lytic triggers reactivated EBV although the combination treatments NaB + TPA and NaB + TGF-β showed the highest induction, with ZEBRA⁺ cells reaching 27.9% and 27.7%,

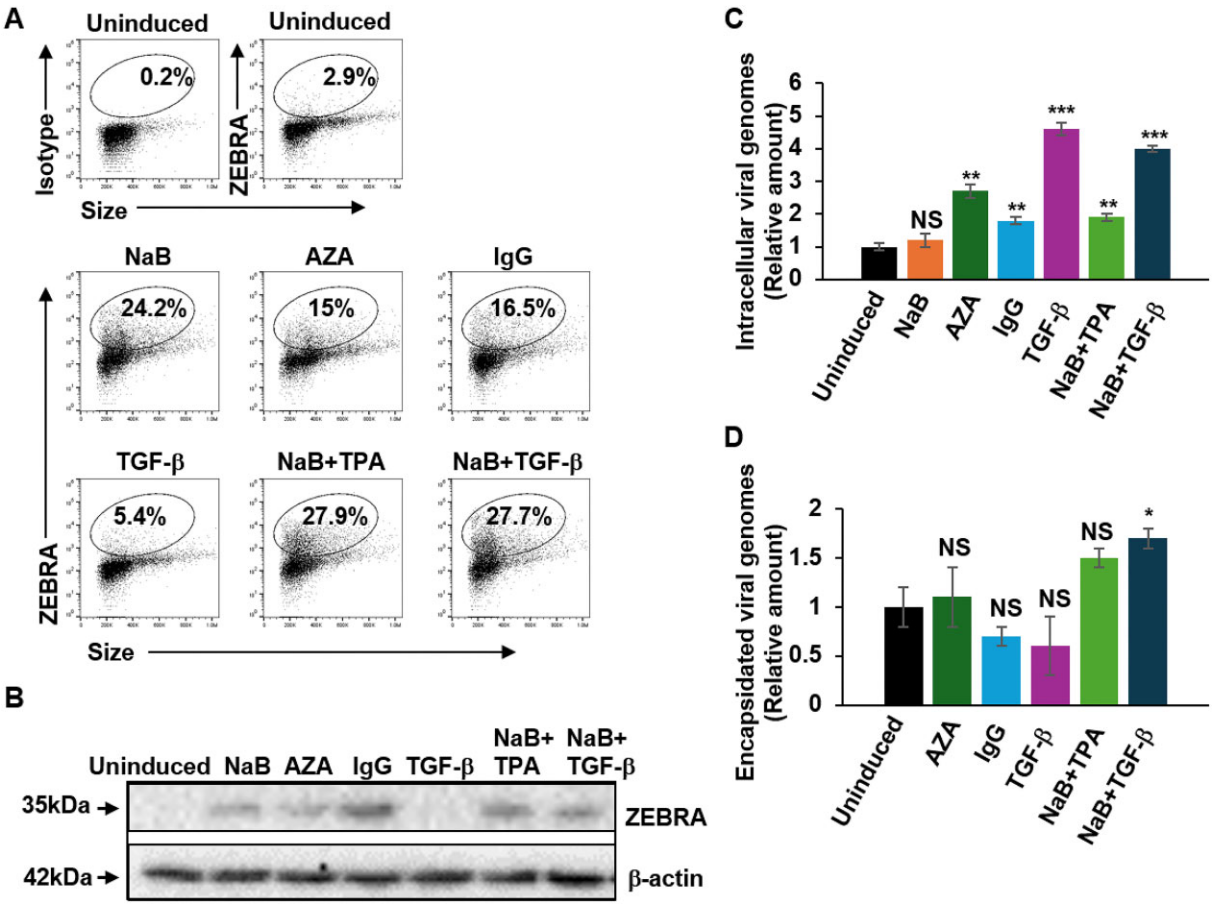

Figure 1. VAL DLBCL supports spontaneous EBV lytic reactivation, with EBV differentially responsive to known lytic triggers, and completing the lytic cycle in response to sodium butyrate plus TGF-β. (**A**, **B**) VAL cells were exposed to several lytic stimuli for 24 h, followed by collection and analysis for ZEBRA$^+$ cells using flow cytometry (**A**) or immunoblotting with the indicated antibodies (**B**). (**C**, **D**) After 48 h of treatment with the specified reagents, VAL cells were collected for qPCR analysis to detect cell-associated viral genomes by amplifying the *BALF5* gene (**C**) or for quantification of released viral genomes after DNase treatment (**D**). These experiments were performed twice; representative results are shown. Error bars, SEM of three technical repeats; $*P < 0.05$; $**P < 0.01$; $***P < 0.001$.

respectively (Fig. 1A). While exposure to IgG demonstrated a stronger response by immunoblotting, responses to the other agents were comparable to those observed by flow cytometry (Fig. 1B). IgG treatment was particularly effective in IBL-1 cells, yielding up to 37.4% ZEBRA$^+$ cells (Fig. 2A), while the other treatments, alone or in combination, did not reactivate EBV (Fig. 2B). In Farage cells, NaB was most effective followed by AZA (14% and 8.4%, respectively). Drug combinations with NaB did not demonstrate greater reactivation by flow cytometry and detection of ZEBRA by immunoblotting was minimal (Fig. 3A and B). In BCKN-1 cells, IgG treatment triggered a pronounced EBV reactivation, demonstrating 36.8% ZEBRA$^+$ cells. In comparison, NaB or TPA induced a modest reactivation (4.7% and 4% ZEBRA$^+$ cells, respectively), while other treatments, including AZA and TGF-β, produced minimal effects (Fig. 4A). Immunoblot results generally aligned with flow cytometry, showing marked ZEBRA expression with IgG or NaB + TPA, indicating that combined treatment is particularly effective in activating the lytic cycle in BCKN-1 cells (Fig. 4B); that said, while NaB and TPA each triggered ~4% lytic cells, immunoblotting only demonstrated ZEBRA expression in response to NaB + TPA. Notably, unlike VAL cells, the other DLBCLs were tightly latent at baseline (Fig. 1A versus Figs 2A, 3A, and 4A).

The lytic phase is frequently abortive in DLBCL cells

To assay progress of the lytic phase following exposure to lytic triggers in VAL cells, we measured intracellular viral genomes using qPCR and found that all lytic triggers and combinations except NaB increased EBV genome copy numbers (Fig. 1C). In contrast, only NaB + TGF-β caused a significant increase in encapsidated viral genomes released into the supernatant, and, while NaB + TPA showed a similar trend, the increase was not significant (Fig. 1D). In the case of IBL-1, aligned with reactivation results shown in Fig. 2A and B, intracellular viral genomes increased only in the IgG treated group (Fig. 2C); this increase resulted in the release of encapsidated virus in the supernatant (Fig. 2D). Because the other lytic stimuli did not trigger viral genome replication, we did not examine the supernatants for released virus. Thus, the IBL-1 DLBCL is tightly latent but EBV reactivates in response to IgG crosslinking and completes the lytic cycle.

In Farage cells, AZA induction uniquely led to an increase in intracellular viral genomes without a corresponding rise in extracellular encapsidated viral load (Fig. 3C, D). This suggests that while AZA effectively stimulates EBV genome replication within the cells, it does not support the subsequent stages of the viral life cycle that lead to the release of infectious particles. On the other hand, the block in lytic phase progres-

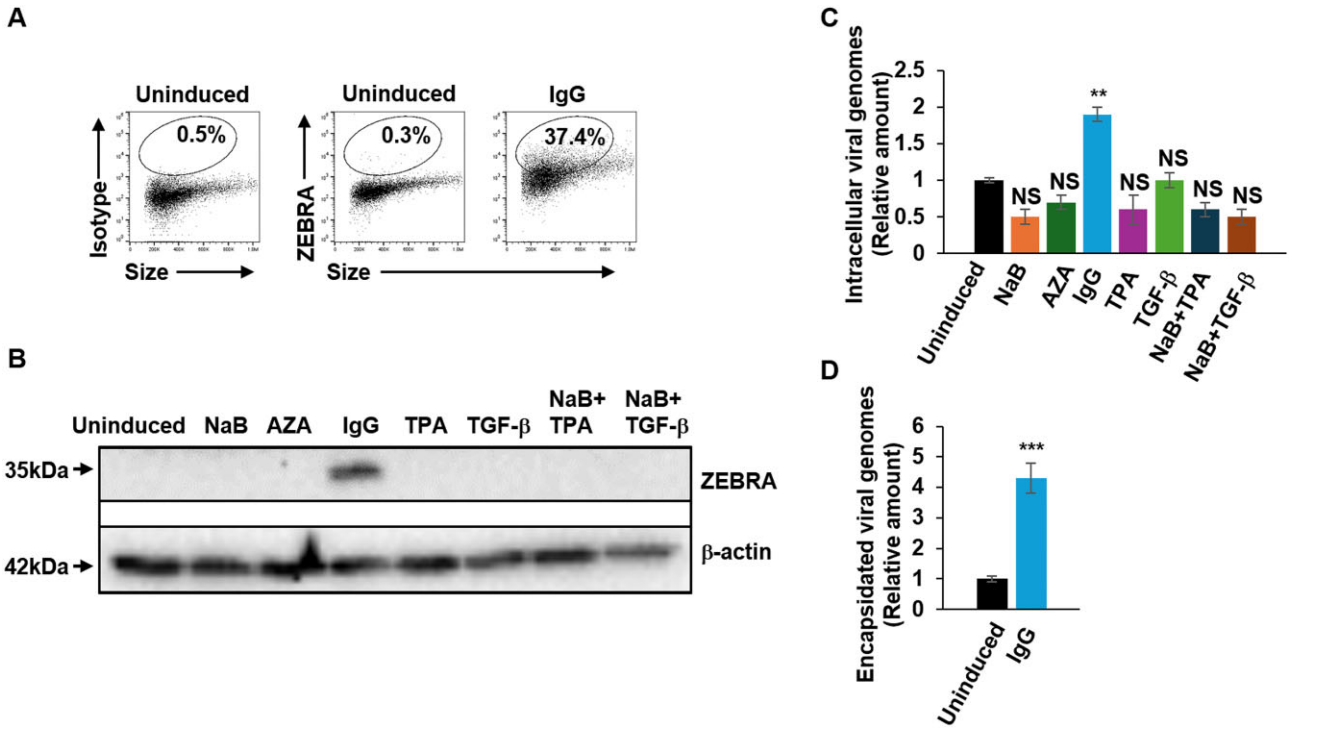

Figure 2. IBL-1 DLBCL is tightly latent but responds to IgG crosslinking by reactivating EBV and completing the lytic cycle. (**A**, **B**) IBL-1 cells were treated with the indicated reagents for 24 h to induce the EBV lytic cycle, then collected for analysis of ZEBRA$^+$ cells via flow cytometry (**A**) or immunostaining with the specified antibodies (**B**). (**C**, **D**) Following a 48-h treatment with the indicated reagents, IBL-1 cells were harvested for qPCR analysis of cell-associated viral genomes by amplifying the *BALF5* gene (**C**) or to measure released viral genomes after DNase treatment (**D**). These experiments were performed twice; representative results are shown. Error bars, SEM of three technical repeats; $^{**}P < 0.01$; $^{***}P < 0.001$.

sion appears to be further upstream for NaB and NaB + TGF-β as ZEBRA expression was not followed by viral genome replication. In BCKN-1 cells, while TPA and NaB + TPA triggered viral genome replication (though not proportional to the amount ZEBRA in Fig. 4A and B), surprisingly, IgG did not despite robust reactivation noted in Fig. 4A and B (Fig. 4C). The other surprise was the very modest though significant increase in genome replication in response to AZA without a substantial increase in ZEBRA$^+$ cells in Fig. 4A (Fig. 4C). Furthermore, none of the lytic stimuli that triggered viral genome replication in BCKN-1 cells drove the lytic phase to completion (Fig. 4D).

Overall, these experiments indicate that while known lytic stimuli variably trigger EBV reactivation in DLBCLs, progress of the lytic phase is frequently blocked early, i.e. upstream of viral genome replication (for example, in response to NaB in VAL, Farage, and BCKN-1 cells) or late, i.e. downstream of genome replication. Only VAL and IBL-1 cells were able to complete the lytic cycle in response to NaB + TGF-β and IgG, respectively.

Lytic triggers upregulate NLRP3 to activate the NLRP3 inflammasome in DLBCL

EBV in latently infected LCL and BL cell lines uses the inflammasome as a security system to alert itself of threats to its home, the B cell. The NLRP3 inflammasome is an intracellular sensor that responds to various stress signals, including reactive oxygen species, lysosomal damage, and electrolyte changes [25, 26]. As a crucial component of the innate immune system, NLRP3 promotes the release of pro-inflammatory cytokines and can even trigger cell death [27]. In EBV$^+$ BL and LCL, the NLRP3 inflammasome initiates EBV's transition from latency to the lytic phase by forming a complex with the thioredoxin interacting protein TXNIP under specific stress conditions, activating caspase-1, which in turn leads to the partial degradation of the heterochromatin-inducing protein KAP1 [13, 14]. This degradation removes KAP1-mediated transcriptional repression of the *BZLF1* (ZEBRA) gene, the EBV replication switch, thus driving the virus into the lytic phase. To investigate if the NLRP3 inflammasome also facilitates EBV lytic reactivation in DLBCL lines, we exposed DLBCLs to NaB (VAL and Farage) or NaB + TPA (BCKN-1) for 24 or 48 h and examined transcript levels of *NLRP3*. We observed a significant elevation of *NLRP3* mRNA after exposure to lytic triggers, suggesting that *NLRP3* is indeed upregulated during lytic reactivation (Fig. 5A), consistent with previous findings in BL cells and LCL. We also observed elevated levels of NLRP3 and TXNIP proteins following exposure of Farage cells to NaB and AZA and BCKN-1 cells to AZA and IgG (Fig. 5B). In addition, compared to control siRNA, knockdown of NLRP3 blocked the cleavage of caspase-1 in VAL (Fig. 5C), Farage (Fig. 5D), and BCKN-1 (Fig. 5E) cells, further supporting that the NLRP3 inflammasome is activated during EBV lytic reactivation in DLBCL cells.

Lytic triggers elevate TXNIP expression leading to inflammasome activation in DLBCL

The role of TXNIP in reactivating EBV has significant implications, as the lytic phase is essential for viral propagation and contributes to oncogenesis [28]. Furthermore, TXNIP's involvement in glucose metabolism links it to metabolic con-

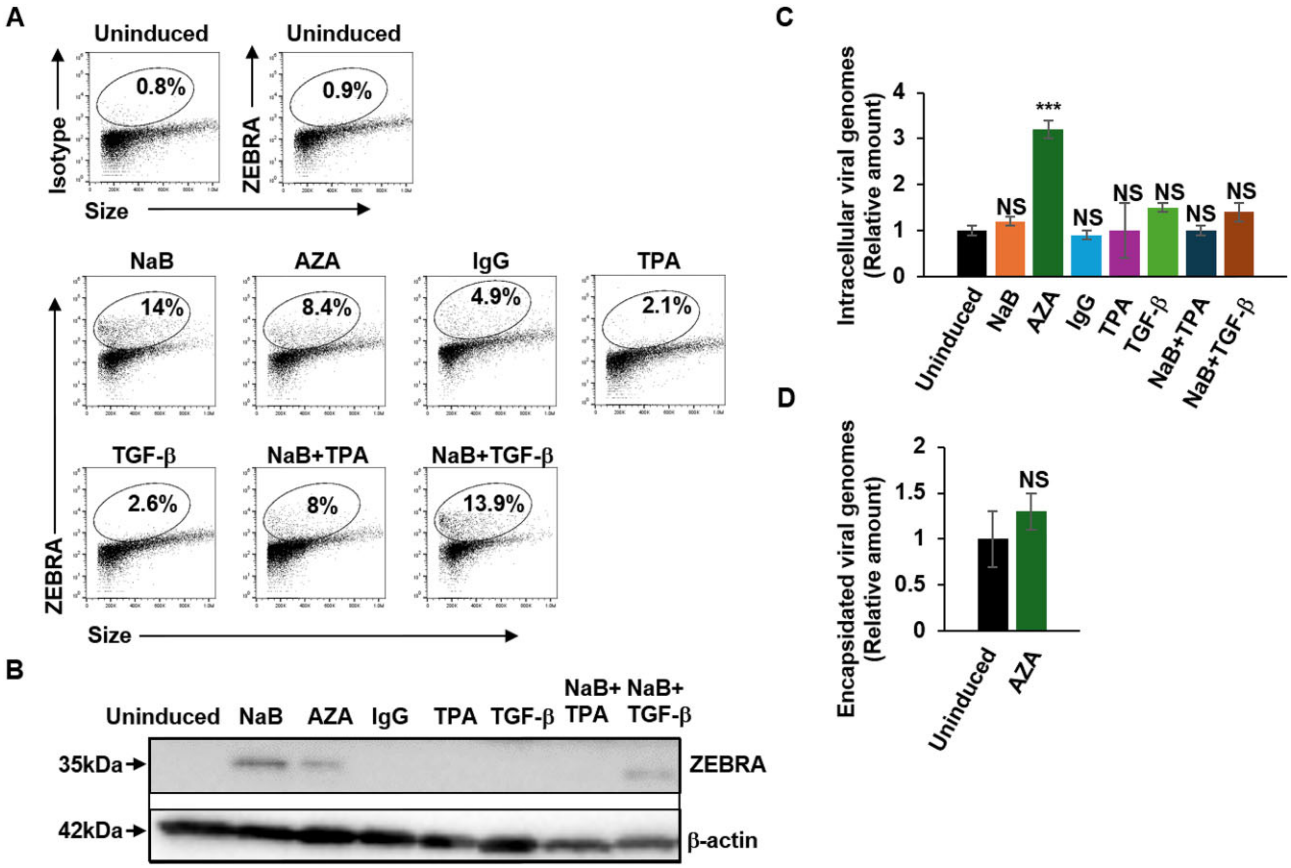

Figure 3. Farage DLBCL is tightly latent but responds to several lytic triggers resulting in an abortive lytic phase. Farage cells were treated with different reagents for 48 h to induce EBV reactivation followed by flow cytometric analysis for ZEBRA$^+$ cells (**A**), immunostaining with the indicated antibodies (**B**), and qPCR analysis of the EBV *BALF5* gene for cell-associated viral genomes (**C**) and DNase resistant viral genomes in the supernatant (**D**). These experiments were performed twice; representative results are shown. Error bars, SEM of three technical repeats; ***$P < 0.001$.

ditions, such as diabetes, which are known to activate the NLRP3 inflammasome [29–31]. Thus, TXNIP serves as a critical mediator in EBV biology by translating metabolic stress signals into inflammasome activation and viral reactivation. Relevant to this and the increased levels of NLRP3 that we observed, we also detected increased TXNIP transcripts in VAL, Farage and BCKN-1 cells after exposure to different lytic stimuli (Fig. 6A). As shown in Fig. 5B, TXNIP protein was also elevated in Farage and BCKN-1 cells after exposure to lytic triggers. In addition, depletion of TXNIP also led to a reduction in cleaved caspase-1 levels in five of six experimental samples across three DLBCL lines (Fig. 6B–D), highlighting TXNIP's pivotal role in activating the inflammasome in these cell types. Thus, the TXNIP-NLRP3 inflammasome is activated in response to lytic stimuli in EBV$^+$ DLBCLs.

The danger sensing NLRP3 inflammasome activates the EBV lytic cycle in DLBCL

We next addressed if the danger-sensing TXNIP-NLRP3 inflammasome was involved in activating the EBV lytic cycle in DLBCLs. Immunoblotting results demonstrated a marked reduction in ZEBRA expression upon NLRP3 or TXNIP knockdown in Farage (Fig. 7A) and VAL (Fig. 7B and C) DLBCLs following lytic induction with NaB (left panels) or AZA (right panels); NLRP3 and TXNIP knockdown were demonstrated in Figs 5B and C, and 6B. MCC950 is a potent and specific inhibitor of the NLRP3 inflammasome that targets the Walker B motif in the NACHT domain of NLRP3, blocking ATP hydrolysis and preventing inflammasome activation [32, 33]. Following treatment with MCC950 and AZA, we observed reduced levels of *BZLF1* transcripts (Fig. 7D) and ZEBRA protein (Fig. 7E) compared to cells induced with AZA alone. Moreover, inhibiting the NLRP3 inflammasome with MCC950 led to a decrease in EBV genome copies (Fig. 7F). Taken together, these findings demonstrate the essential role of the danger sensing TXNIP-NLRP3 inflammasome in EBV lytic activation in DLBCL cells.

The danger sensing UPR activates NLRP3 inflammasome components to reactivate EBV in DLBCL

XBP1, a key transcription factor activated by the UPR, has been reported to reactivate EBV in epithelial cells and LCL [34]. The UPR inducing agent Bortezomib has also been shown to activate the EBV lytic cycle in BL cells [35]. Since the UPR/ER stress, like the inflammasome, senses danger, we assessed the influence of UPR and the XBP1 pathway on EBV reactivation in VAL cells. Tunicamycin, an ER stress inducer [36], was used together with 4μ8C, an ER stress inhibitor [37, 38], followed by NaB treatment to stimulate EBV lytic cycle activation. Flow cytometry analysis demonstrated that Tunicamycin increased the percentage of ZEBRA$^+$ cells, indicating enhanced EBV lytic reactivation, while 4u8C reduced the frequency of ZEBRA$^+$ cells (Fig. 8A and B). We also found that

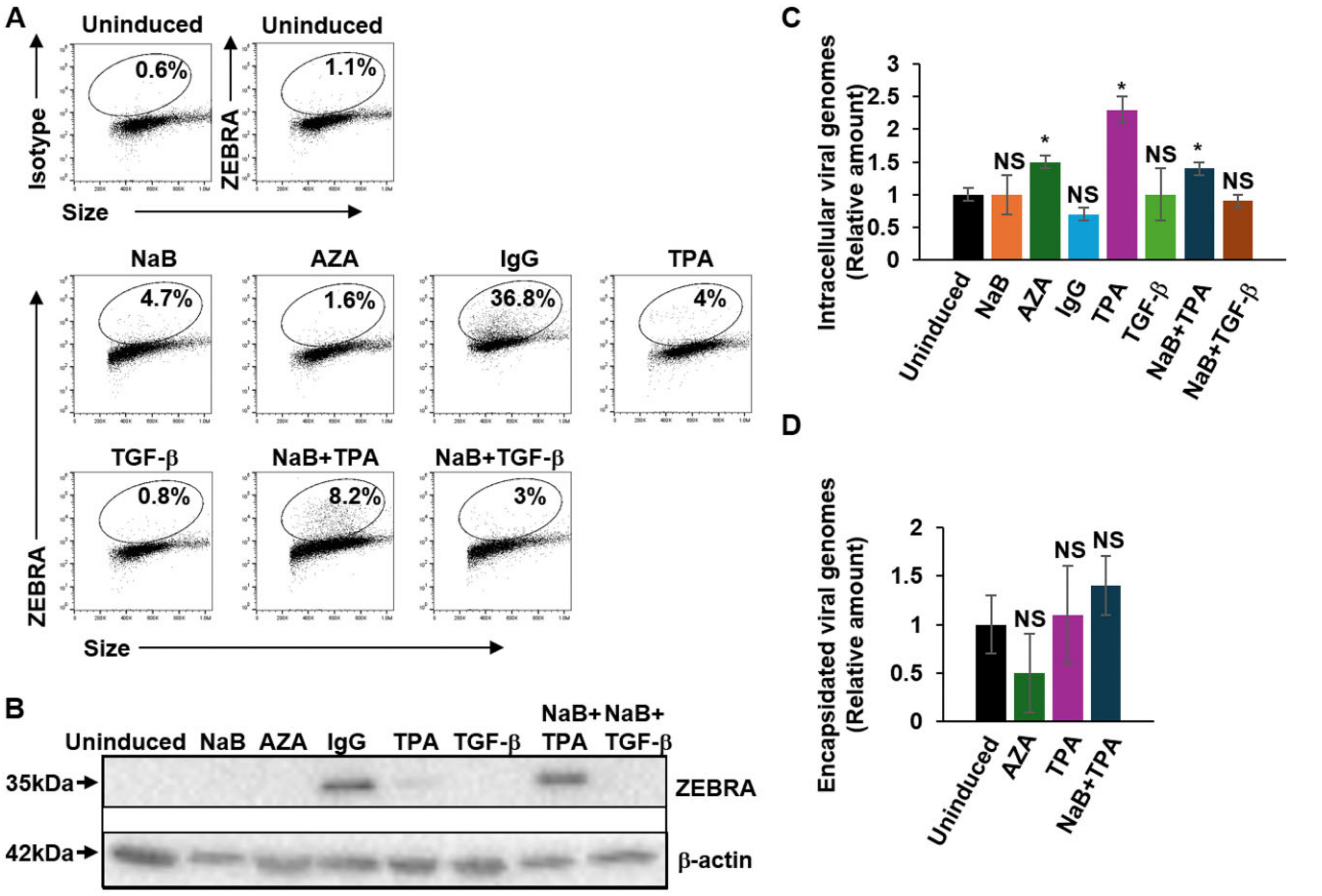

Figure 4. Tightly latent BCKN-1 DLBCL responds robustly to some lytic triggers but does not support the complete lytic cycle. BCKN-1 cells were exposed to the indicated reagents for 48 h followed by flow cytometric analysis for ZEBRA$^+$ cells (**A**), immunostaining with the indicated antibodies (**B**), and qPCR analysis of the EBV *BALF5* gene for cell-associated viral genomes (**C**) and DNase resistant viral genomes in the supernatant (**D**). These experiments were performed twice; representative results are shown. Error bars, SEM of three technical repeats; $*P < 0.05$.

following exposure to lytic stimuli, the abundance of XBP1S increased rapidly, i.e. by 3 h, and preceded the expression of ZEBRA, around 9–12 h (Fig. 8C). The upregulation of XBP1S was accompanied by a parallel increase in NLRP3 protein by 6 to 9 h (Fig. 8C). These results indicate that ER stress, via XBP1 activity, may promote EBV reactivation in DLBCL. To examine the role of XBP1, we performed knockdown experiments, targeting the coding region (si*XBP1* #1) or 3′ UTR (si*XBP1* #2) of the *XBP1* gene. RT-qPCR analysis showed a reduction in both *NLRP3* and *TXNIP* transcripts upon *XBP1* knockdown (Fig. 8D), implicating XBP1 in the regulation of these inflammasome-associated genes. Additionally, immunoblot analysis revealed that NLRP3 and ZEBRA expression decreased when *XBP1* was knocked down (Fig. 8E). These findings indicate that ER stress and XBP1 may facilitate EBV activation in DLBCL by upregulating NLRP3 and TXNIP.

To confirm the specific role of XBP1 in EBV reactivation, we performed a rescue experiment by reintroducing the spliced form of XBP1 (XBP1S) in XBP1 knockdown cells. RT-qPCR analysis confirmed knockdown and rescued levels of XBP1 in VAL cells before induction by NaB (Fig. 8F, left panel). Overexpression of XBP1S resulted in a 2-fold increase in *BZLF1* transcripts, whereas depleting XBP1 did not affect *BZLF1* transcript levels in cells without lytic induction (Fig. 8F, right panel). Following NaB exposure, XBP1S overexpression in the setting of XBP1 depletion increased the frequency of ZEBRA$^+$ cells from 7.2% to 11.6%, i.e. by 60%, restoring the EBV reactivation rate to almost the baseline level of 12.6%; furthermore, overexpression of XBP1S nearly doubled the frequency of ZEBRA$^+$ cells from 12.6% to 23.3% (Fig. 8G and H). This rescue effect underscores the role of XBP1S in enhancing EBV reactivation through its regulatory influence on ZEBRA expression, supporting our hypothesis that XBP1S, potentially via NLRP3 and TXNIP, is integral to the ER stress-mediated pathway facilitating EBV lytic activation.

EBV lytic cycle inducers in combination with the nucleoside analog ganciclovir enhance cell killing of EBV$^+$ DLBCL

To analyze the effects of different treatments on cell viability, we treated VAL and the EBV$^-$ DLBCL line SUDHL6 with AZA, AZA plus ganciclovir (GCV), or GCV alone, and used DMSO (uninduced) as a control. IBL-1 cells were treated with DMSO (uninduced), GCV, IgG, and IgG + GCV, followed by flow cytometry to count live and dead cells. In both EBV$^+$ cell lines, an important consideration was whether the selected lytic trigger resulted in the progress of the lytic phase beyond expression of ZEBRA. As shown earlier, AZA and IgG caused increased viral genome replication in VAL and IBL-1 cells, respectively (Figs 1C and 2C), assuring us of early gene

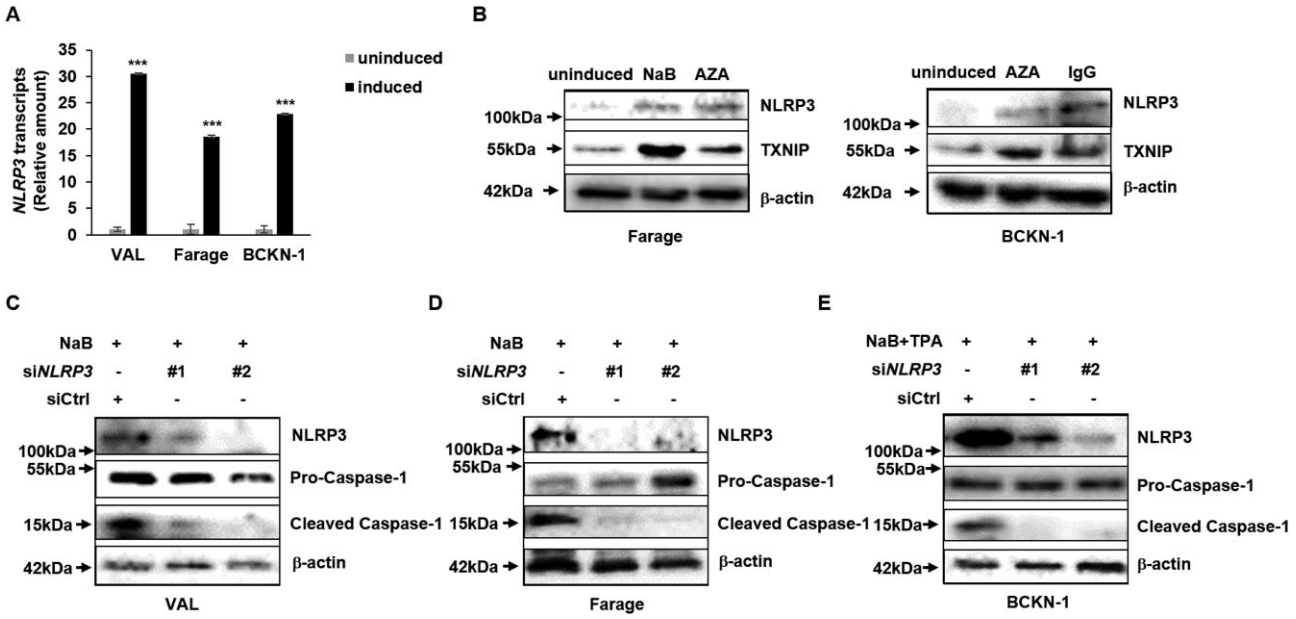

Figure 5. Lytic triggers upregulate NLRP3 to activate the inflammasome in DLBCL lines. (**A**) VAL, Farage, and BCKN-1 cells were treated with NaB (VAL and Farage) or NaB + TPA (BCKN-1) for 24 (VAL) or 48 h (Farage and BCKN-1). Cells were harvested and analyzed for *NLRP3* expression using RT-qPCR. (**B**) Farage and BCKN-1 cells were treated with NaB, AZA (Farage) or AZA and IgG (BCKN-1) for 24 h. Cells were harvested and analyzed for NLRP3 and TXNIP expression using immunoblotting. (**C**–**E**) VAL (**C**), Farage (**D**), and BCKN-1 (**E**) cells were transfected with either control siRNA (siCtrl) or siRNA targeting *NLRP3* (si*NLRP3* #1, #2). After 20 h, the cells were exposed to NaB or NaB + TPA, harvested after an additional 6 h (VAL) or 24 h (Farage and BCKN-1), and analyzed by immunoblotting with the indicated antibodies. These experiments were performed three times; representative results are shown. Error bars, SEM of three technical repeats; $***P < 0.001$.

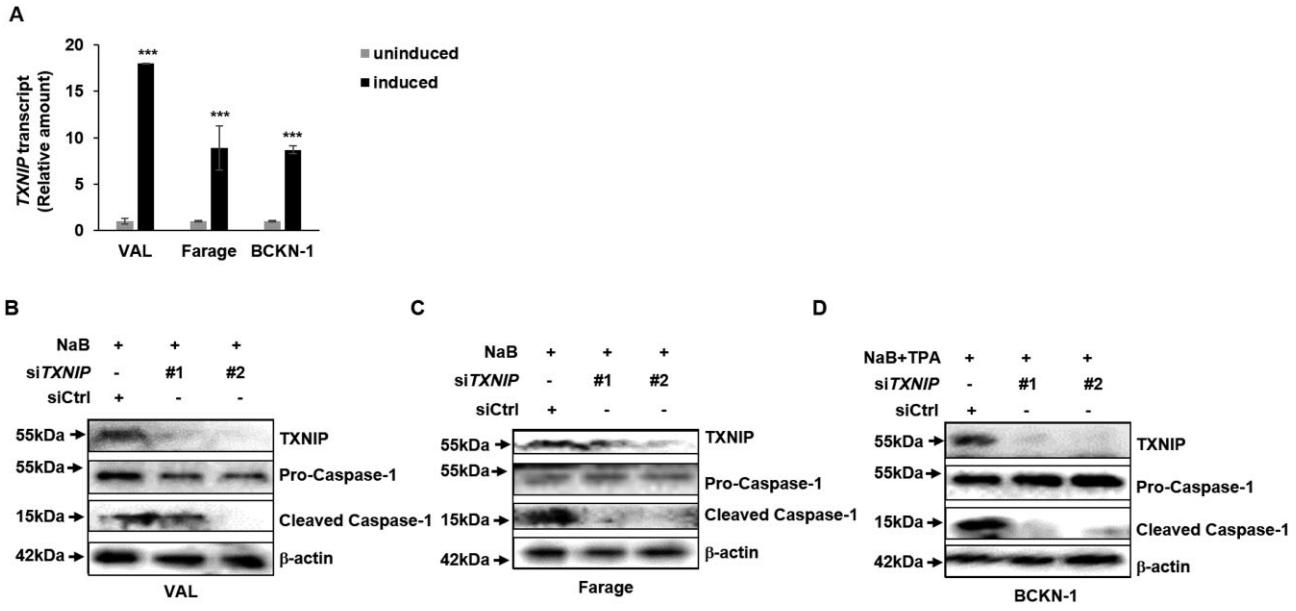

Figure 6. Lytic triggers upregulate TXNIP to activate the inflammasome in DLBCL lines. (**A**) VAL, Farage, and BCKN-1 cells were induced with NaB (VAL and Farage) or NaB + TPA (BCKN-1) for 24 h (VAL) or 48 h (Farage and BCKN-1). Following harvest, cells were subjected to RT-qPCR analysis of *TXNIP*. (**B**–**D**) VAL (**B**), Farage (**C**), and BCKN-1 (**D**) cells were transfected with control siRNA (siCtrl) or siRNA targeting *TXNIP* (si*TXNIP* #1, #2). After 20 h, the cells were exposed to NaB or NaB + TPA, harvested after an additional 6 h (VAL) or 24 h (Farage and BCKN-1), and immunoblotted with the indicated antibodies. These experiments were performed three times; representative results are shown. Error bars, SEM of three technical repeats; $***P < 0.001$.

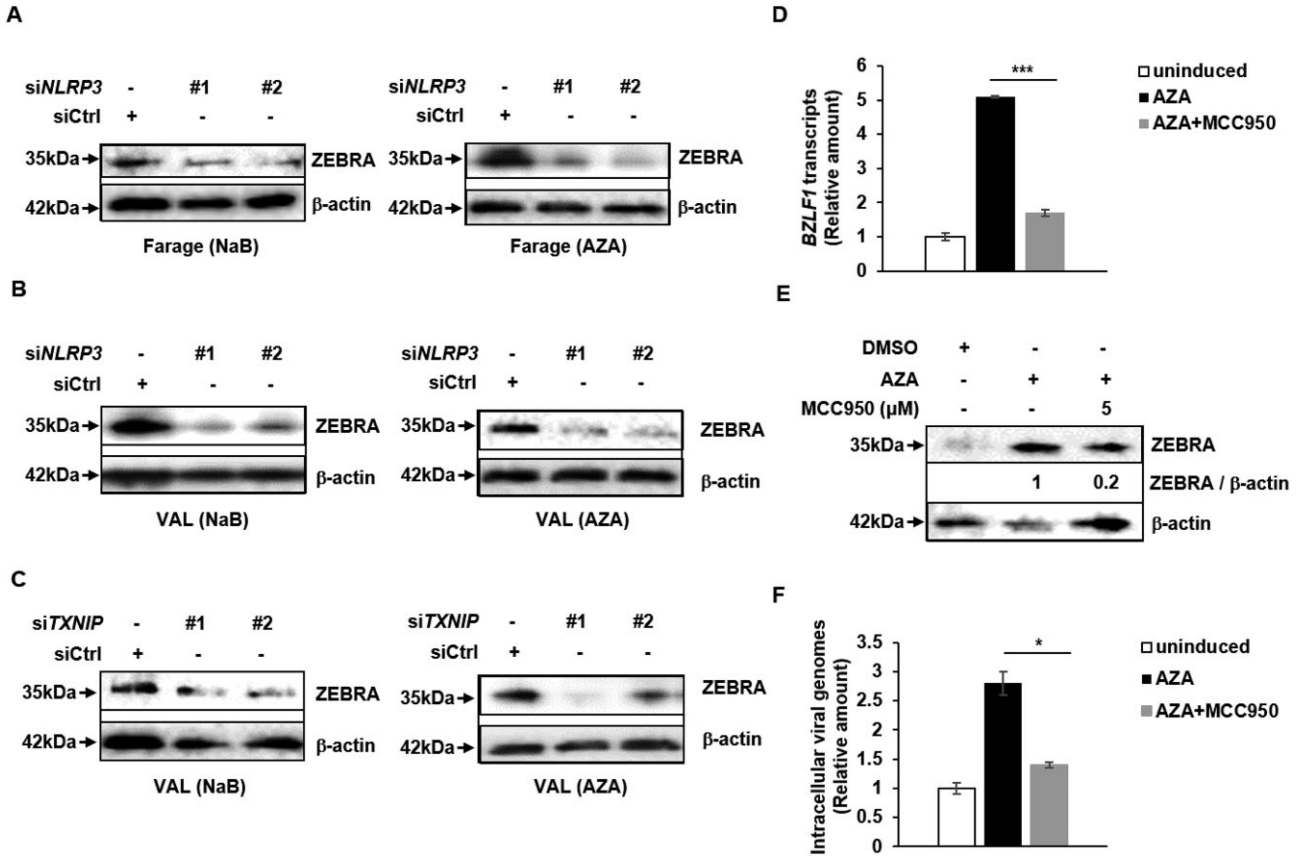

Figure 7. The danger sensing NLRP3 inflammasome activates the EBV lytic cycle in DLBCLs. (**A**, **B**) Farage (**A**) and VAL (**B**) cells were transfected with control siRNA (siCtrl) or siRNA targeting *NLRP3* (si*NLRP3* #1, #2). After 20 h, cells were treated with NaB (left panel) or AZA (right panel), harvested after an additional 48 h (Farage) or 24 h (VAL), and analyzed by immunoblotting with the indicated antibodies. (**C**) VAL cells were transfected with siCtrl or siRNA targeting *TXNIP* (si*TXNIP* #1, #2), exposed to NaB (left panel) or AZA (right panel) after 20 h, and harvested after another 24 h for immunoblotting. (**D**–**F**) VAL cells were treated with AZA with or without 5 μM MCC950 for 24 (**D**, **E**) or 48 h (**F**). Following harvest, cells were subjected to RT-qPCR analysis for *BZLF1* transcripts (**D**), immunoblotting with the indicated antibodies (**E**), or qPCR analysis of cell-associated viral genomes by amplifying the *BALF5* gene (**F**). These experiments were performed twice; representative results are shown. Error bars, SEM of three technical repeats; $*P < 0.05$; $***P < 0.001$.

(including *BGLF4*) expression which is known to be kinetically and functionally upstream of viral genome replication. *BGLF4* encodes the key viral protein kinase necessary for GCV activation. In all three cell types, GCV treatment alone did not significantly alter the number of live cells compared to solvent treated cells (Fig. 9A–F). However, while treatment with a lytic inducing agent for a week caused cell death in both VAL and SUDHL6, the level of significance was greater for the EBV$^+$ line VAL compared to the EBV− line SUDHL6 ($P < 0.001$ versus $P < 0.05$; Fig. 9A and C). Furthermore, enhanced cell death was only observed when GCV was added to the two EBV$^+$ DLBCL lines (Fig. 9A, B, D, and E) compared to the EBV$^-$ line SUDHL6 (Fig. 9C and F) implicating the presence of EBV in enhanced cell killing. To further validate the mechanism underlying enhanced cell death upon GCV treatment, we quantified *BGLF4* expression. Following exposure to lytic triggers, *BGLF4* transcript levels were significantly upregulated in VAL, Farage, IBL-1, and BCKN-1 cells (Fig. 9G). This indicates that lytic reactivation in DLBCLs promotes sufficient *BGLF4* expression, thereby enabling GCV to exert enhanced cytotoxic effects. These results support oncolytic killing by incorporation of a toxic nucleoside analog in DLBCL cells supporting the EBV lytic phase.

Taken together, our findings highlight the complex and variable responses of EBV$^+$ DLBCL cells to different lytic inducers, with the UPR and the NLRP3 inflammasome pathways intersecting to influence reactivation outcomes across cell lines.

Discussion

This study provides a foundational understanding of the EBV lytic phase in DLBCLs, including the stimuli that trigger the lytic cycle, the characteristics of the lytic phase induced by these stimuli, and some of the underlying mechanisms driving the response. At baseline, EBV remains tightly latent in three of the four cell lines, similar to most lymphoblastoid cell lines. While all the lines respond to lytic stimuli to varying extents, the majority of cases result in an abortive lytic phase. Notably, exceptions where the lytic cycle progresses to the release of encapsidated viral particles include the response of VAL cells to NaB plus TGF-β and that of IBL-1 cells to IgG. These differences highlight the complex regulation of EBV reactivation in different EBV$^+$ DLBCLs and suggest that cell line/tumor-specific factors influence the outcome.

Mechanistically, linking the activation of two innate danger-sensing pathways enables a two-pronged approach for inducing *BZLF1* expression. XBP1S promotes transcription of NLRP3 components, leading to inflammasome activation, which in turn removes silencing factors from the *BZLF1* promoter; simultaneously, XBP1 directly activates the *BZLF1*

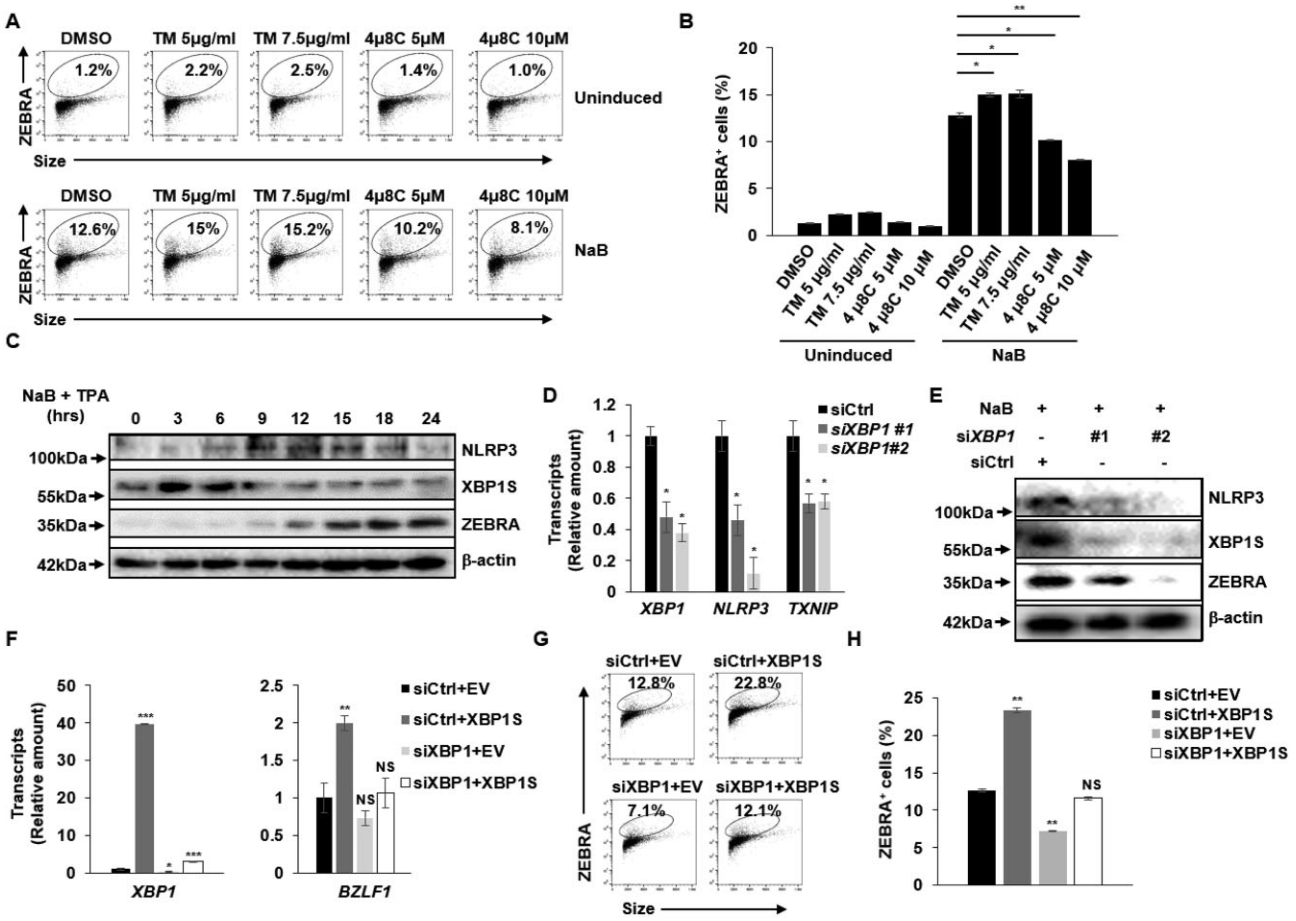

Figure 8. The danger sensing UPR activates NLRP3 inflammasome components and the EBV lytic cycle in DLBCL. (**A** and **B**) VAL cells were pre-incubated with different concentrations of tunicamycin (TM) or 4μ8C for 2 h and then left untreated or treated with NaB for another 24 h. Cells were analyzed for ZEBRA expression by flow cytometry (**A**). Aggregate data from biological triplicates of the experiment in A are presented in B. (**C**) VAL cells were exposed to NaB + TPA for different lengths of time and collected for immunoblotting. (**D**, **E**) VAL cells were transfected with control siRNA (siCtrl) or siRNA targeting *XBP1* (si*XBP1* #1, #2). After 20 h, cells were collected for RT-qPCR analysis of *XBP1*, *NLRP3* and *TXNIP* transcripts (**D**), or induced with NaB for another 24 h for immunoblotting (**E**). (**F**–**H**) VAL cells were transfected with siCtrl + empty vector (EV), siCtrl + XBP1S plasmid, si*XBP1* + EV or si*XBP1* + XBP1S plasmid. Twenty-four hours later, cells were collected for RT-qPCR analysis of *XBP1* and *BZLF1* transcripts (**F**), or induced with NaB for another 24 h and collected for flow cytometry analysis (**G**). (**H**) Aggregate data of ZEBRA$^+$ cells from biological triplicates of the experiment in panel (G) are presented in panel (H). Error bars, SEM; $*P < 0.05$; $**P < 0.01$; $***P < 0.001$.

promoter, thereby suppressing pro-latent forces and exerting pro-lytic forces at the same time. This coordinated dual approach likely serves as a safety mechanism to regulate the magnitude of the lytic response, promoting viral persistence. This argument is supported by (i) the finding that DLBCLs are tightly latent and (ii) knockdown of either of these innate pathways markedly reduces lytic reactivation. While both pathways can be activated by damage and pathogen associated molecular patterns, connecting the two pathways, XBP1S was found to enhance the activity of the NLRP3 promoter in a reporter assay; furthermore, studies in mice have shown that tissue injury links XBP1S to the transcriptional activation of NLRP3 [39, 40]. As for TXNIP, while XBP1S may transcriptionally activate TXNIP, the UPR may contribute to TXNIP abundance by other means. XBP1 is activated to the transcription factor XBP1S via splicing in part mediated by the ER stress response/UPR regulatory protein and endoribonuclease IRE1α. IRE1α activation results in degradation of transcripts. Of relevance to our findings, miRNA degradation caused by IRE1α has been linked to loss of the miR17 and de-repression of TXNIP translation [41].

Reactivation of EBV in BL cells and LCL typically leads to a full lytic cycle [14, 20, 42–44]. Therefore, the predominantly abortive response observed in DLBCL cells to most lytic triggers is unexpected. Our observations revealed that the lytic cycle in DLBCLs can be aborted either early—prior to viral genome replication—or late—after genome replication, without subsequent virus release. The reasons behind this abortive lytic cycle in DLBCL remain unclear, although several potential factors may contribute. One possibility is that certain lytic stimuli are particularly toxic to DLBCLs; for instance, NaB, an HDAC inhibitor commonly used as a single agent to reactivate EBV in other EBV-positive lymphoma cells, failed to trigger a complete lytic cycle in all DLBCL lines tested. Another potential factor is the limited extent of viral genome replication, which was only 3–5-fold over baseline (Figs 1–4), potentially restricting packaging and release of virions. A third possibility is a low number of viral episomes per cell, which could hinder robust genome replication—this contrasts with the >25-fold replication observed in BL cells [45]. Nonetheless, as long as the lytic cycle is aborted at the late stage, DLBCLs may still be vulnerable to enhanced toxicity from ganciclovir. Indeed, we

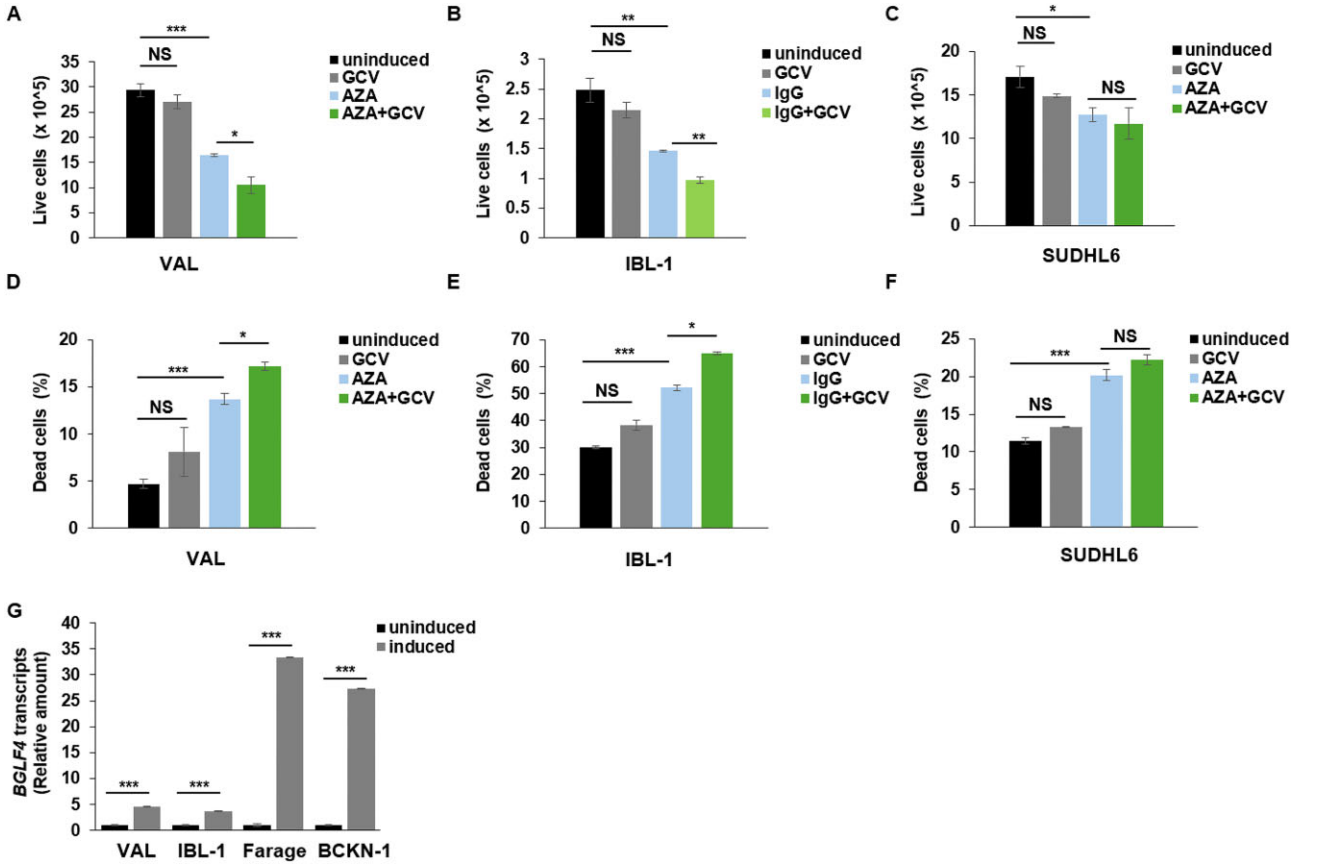

Figure 9. Lytic cycle activators enhance oncolytic death of DLBCLs in the presence of a nucleoside analog. EBV$^+$ DBCL lines VAL (**A**, **D**) and IBL-1 (**B**, **E**), and EBV$^-$ DLBCL line SUDHL6 (**C**, **F**) cells were incubated with the specified reagents together with/without GCV for 168 h (VAL and SUDHL6) or 96 h (IBL-1). Medium with fresh GCV was replaced every 48 h for the groups where GCV was added at the beginning. Live and dead cells were enumerated by PI staining and flow cytometry. Error bars, SEM from biological triplicates; $*P < 0.05$; $**P < 0.01$; $***P < 0.001$. (**G**) VAL, IBL-1, Farage, and BCKN-1 cells were induced with NaB (VAL and Farage), IgG (IBL-1), or NaB + TPA (BCKN-1) for 24 h (VAL and IBL-1) or 48 h (Farage and BCKN-1). Following harvest, cells were subjected to RT-qPCR analysis of *BGLF4*. Error bars, SEM of three technical repeats; $***P < 0.001$; this experiment was performed twice.

observed increased cell death in VAL cells exposed to ganciclovir, even when a late abortive lytic phase was triggered by AZA.

Our experiments explored two contrasting therapeutic strategies. The first, an antiviral approach, involved the use of MCC950 to inhibit EBV reactivation. MCC950 works by blocking the activation of the NLRP3 inflammasome, specifically inhibiting its ATP hydrolysis activity [32, 33]. As a small molecule, MCC950 has shown promise in preclinical models of inflammatory, autoimmune, cardiovascular, and metabolic diseases [46]. Although MCC950 did not progress beyond a Phase I safety trial, several other NLRP3 inhibitors have advanced to Phase II and III trials [47]. By preventing or limiting EBV-induced B cell transformation, this antiviral strategy could benefit immunosuppressed individuals at high risk for developing EBV-related cancers. The second approach is an oncolytic strategy, which aims to activate the EBV lytic cycle in tumor cells to induce virus-driven cell death. As mentioned previously, EBV lytic cycle in DLBCL cells is typically abortive, with rare virion release into the extracellular environment. This incomplete reactivation may offer clinical advantages by minimizing the risk of widespread EBV dissemination while still triggering cell death pathways. Controlled lytic reactivation could also enhance tumor cell susceptibility to immune-mediated clearance and antiviral therapies like ganciclovir, which specifically targets cells undergoing lytic replication [9, 48, 49]. Ganciclovir, a widely used prodrug, targets actively replicating genomes. Upon entry into EBV-infected cells, ganciclovir is phosphorylated by a viral kinase expressed only during the lytic phase, converting it into an active form that incorporates into replicating viral DNA, ultimately causing toxicity to the infected cancer cells [50].

While clinically available drugs that target the UPR and the NLRP3 inflammasome are not yet readily available, our study highlights the importance of efforts to develop such agents. Integrating EBV lytic induction therapy into current treatment strategies for EBV$^+$ DLBCL could significantly increase tumor sensitivity to agents like ganciclovir, offering a more targeted approach for managing this aggressive malignancy. Understanding the disparate responses to lytic triggers and the mechanisms driving EBV lytic reactivation in DLBCL will facilitate the development of novel inducers and inhibitors with enhanced specificity for EBV$^+$ DLBCL, and potentially different DLBCL subtypes, ultimately broadening treatment options for EBV-associated cancers.

Acknowledgements

Author contributions: H.X.: conceptualization, methodology, validation, formal analysis, investigation, data curation, visualization, writing - original draft; T.E.H.: investigation, formal analysis; S.K.: investigation, formal analysis; B.A.R.:

investigation; D.X.: investigation; M.T.M.: conceptualization, methodology, validation, formal analysis, data curation, visualization, supervision, project administration, funding acquisition; S.B.M.: conceptualization, methodology, validation, formal analysis, data curation, visualization, supervision, project administration, funding acquisition, writing - review and editing.

Conflict of interest

The authors have declared that no competing interests exist.

Funding

M.T.M. was supported by the Children's Miracle Network, the National Institutes of Health (grants U01 CA275310 and R01 DE032623), and the United States Department of Agriculture-Animal & Plant Health Inspection Service (contract 6000027242); S.B.M. was supported by the Children's Miracle Network and the National Institutes of Health (grants U01 CA275310 and R01 DE032623).

Data availability

All data supporting the conclusions are presented in the manuscript. There are no large datasets associated with this work.

References

1. Susanibar-Adaniya S, Barta SK. 2021 Update on Diffuse large B cell lymphoma: a review of current data and potential applications on risk stratification and management. *Am J Hematol* 2021;**96**:617–42. https://doi.org/10.1002/ajh.26151
2. Song CG, Huang JJ, Li YJ *et al.* Epstein–Barr virus-positive diffuse large B-cell lymphoma in the elderly: a matched case-control analysis. *PLoS One* 2015;**10**:e0133973. https://doi.org/10.1371/journal.pone.0133973
3. Uner A, Akyurek N, Saglam A *et al.* The presence of Epstein–Barr virus (EBV) in diffuse large B-cell lymphomas (DLBCLs) in Turkey: special emphasis on 'EBV-positive DLBCL of the elderly.'. *APMIS* 2011;**119**:309–16. https://doi.org/10.1111/j.1600-0463.2011.02736.x
4. Malpica L, Marques-Piubelli ML, Beltran BE *et al.* EBV-positive diffuse large B-cell lymphoma, not otherwise specified: 2022 update on diagnosis, risk-stratification, and management. *Am J Hematol* 2022;**97**:951–65. https://doi.org/10.1002/ajh.26579
5. Carbone A, Vaccher E, Gloghini A. Hematologic cancers in individuals infected by HIV. *Blood* 2022;**139**:995–1012. https://doi.org/10.1182/blood.2020005469
6. Chao C, Silverberg MJ, Martinez-Maza O *et al.* Epstein–Barr virus infection and expression of B-cell oncogenic markers in HIV-related diffuse large B-cell lymphoma. *Clin Cancer Res* 2012;**18**:4702–12. https://doi.org/10.1158/1078-0432.CCR-11-3169
7. Dunleavy K, Wilson WH. How I treat HIV-associated lymphoma. *Blood* 2012;**119**:3245–55. https://doi.org/10.1182/blood-2011-08-373738
8. Noy A. Optimizing treatment of HIV-associated lymphoma. *Blood* 2019;**134**:1385–94. https://doi.org/10.1182/blood-2018-01-791400
9. Haverkos B, Alpdogan O, Baiocchi R *et al.* Targeted therapy with nanatinostat and valganciclovir in recurrent EBV-positive lymphoid malignancies: a phase 1b/2 study. *Blood Adv* 2023;**7**:6339–50. https://doi.org/10.1182/bloodadvances.2023010330
10. Damania B, Kenney SC, Raab-Traub N. Epstein–Barr virus: biology and clinical disease. *Cell* 2022;**185**:3652–70. https://doi.org/10.1016/j.cell.2022.08.026
11. Chabay P. Advances in the pathogenesis of EBV-associated diffuse large B cell lymphoma. *Cancers (Basel)* 2021;**13**:2717. https://doi.org/10.3390/cancers13112717
12. Cohen M, Vistarop AG, Huaman F *et al.* Epstein–Barr virus lytic cycle involvement in diffuse large B cell lymphoma. *Hematol Oncol* 2018;**36**:98–103. https://doi.org/10.1002/hon.2465
13. Bhaduri-McIntosh S, Rousseau BA. KAP1/TRIM28 – antiviral and proviral protagonist of herpesvirus biology. *Trends Microbiol* 2024;**32**:1179–89. https://doi.org/10.1016/j.tim.2024.05.007
14. Burton EM, Goldbach-Mansky R, Bhaduri-McIntosh S. A promiscuous inflammasome sparks replication of a common tumor virus. *Proc Natl Acad Sci USA* 2020;**117**:1722–30. https://doi.org/10.1073/pnas.1919133117
15. Willman GH, Xu H, Zeigler TM *et al.* Polymerase theta is a synthetic lethal target for killing Epstein–Barr virus lymphomas. *J Virol* 2024;**98**:e0057224. https://doi.org/10.1128/jvi.00572-24
16. Frey TR, Brathwaite J, Li X *et al.* Nascent transcriptomics reveal cellular prolytic factors upregulated upstream of the latent-to-lytic switch protein of Epstein–Barr Virus. *J Virol* 2020;**94**:e01966-19.https://doi.org/10.1128/JVI.01966-19
17. Xu H, Li X, Rousseau BA *et al.* IFI16 Partners with KAP1 to maintain Epstein–Barr virus latency. *J Virol* 2022;**96**:e0102822. https://doi.org/10.1128/jvi.01028-22
18. Zeng L, Zampetaki A, Margariti A *et al.* Sustained activation of XBP1 splicing leads to endothelial apoptosis and atherosclerosis development in response to disturbed flow. *Proc Natl Acad Sci USA* 2009;**106**:8326–31. https://doi.org/10.1073/pnas.0903197106
19. Xu H, Akinyemi IA, Haley J *et al.* ATM, KAP1 and the Epstein–Barr virus polymerase processivity factor direct traffic at the intersection of transcription and replication. *Nucleic Acids Res* 2023;**51**:11104–22. https://doi.org/10.1093/nar/gkad823
20. Yiu SPT, Dorothea M, Hui KF *et al.* Lytic induction therapy against Epstein–Barr Virus-associated malignancies: past, present, and future. *Cancers (Basel)* 2020;**12**:2142. https://doi.org/10.3390/cancers12082142
21. Gradoville L, Kwa D, El-Guindy A *et al.* Protein kinase C-independent activation of the Epstein–Barr virus lytic cycle. *J Virol* 2002;**76**:5612–26. https://doi.org/10.1128/JVI.76.11.5612-5626.2002
22. Iempridee T, Das S, Xu I *et al.* Transforming growth factor beta-induced reactivation of Epstein–Barr virus involves multiple Smad-binding elements cooperatively activating expression of the latent-lytic switch BZLF1 gene. *J Virol* 2011;**85**:7836–48. https://doi.org/10.1128/JVI.01197-10
23. Liang CL, Chen JL, Hsu YP *et al.* Epstein–Barr virus BZLF1 gene is activated by transforming growth factor-beta through cooperativity of Smads and c-jun/c-Fos proteins. *J Biol Chem* 2002;**277**:23345–57. https://doi.org/10.1074/jbc.M107420200
24. Takada K, Ono Y. Synchronous and sequential activation of latently infected Epstein–Barr virus genomes. *J Virol* 1989;**63**:445–9. https://doi.org/10.1128/jvi.63.1.445-449.1989
25. Swanson KV, Deng M, Ting JP. The NLRP3 inflammasome: molecular activation and regulation to therapeutics. *Nat Rev Immunol* 2019;**19**:477–89. https://doi.org/10.1038/s41577-019-0165-0
26. Bhaduri-McIntosh S, McIntosh MT. Inflammasome, the constitutive heterochromatin machinery, and replication of an oncogenic herpesvirus. *Viruses* 2021;**13**:846. https://doi.org/10.3390/v13050846
27. Paik S, Kim JK, Silwal P *et al.* An update on the regulatory mechanisms of NLRP3 inflammasome activation. *Cell Mol Immunol* 2021;**18**:1141–60. https://doi.org/10.1038/s41423-021-00670-3
28. Munz C. Latency and lytic replication in Epstein–Barr virus-associated oncogenesis. *Nat Rev Micro* 2019;**17**:691–700. https://doi.org/10.1038/s41579-019-0249-7

29. Zhou R, Tardivel A, Thorens B *et al.* Thioredoxin-interacting protein links oxidative stress to inflammasome activation. *Nat Immunol* 2010;**11**:136–40. https://doi.org/10.1038/ni.1831
30. Choi EH, Park SJ. TXNIP: a key protein in the cellular stress response pathway and a potential therapeutic target. *Exp Mol Med* 2023;**55**:1348–56. https://doi.org/10.1038/s12276-023-01019-8
31. Parikh H, Carlsson E, Chutkow WA *et al.* TXNIP regulates peripheral glucose metabolism in humans. *PLoS Med* 2007;**4**:e158. https://doi.org/10.1371/journal.pmed.0040158
32. Coll RC, Hill JR, Day CJ *et al.* MCC950 directly targets the NLRP3 ATP-hydrolysis motif for inflammasome inhibition. *Nat Chem Biol* 2019;**15**:556–9. https://doi.org/10.1038/s41589-019-0277-7
33. Coll RC, Robertson AA, Chae JJ *et al.* A small-molecule inhibitor of the NLRP3 inflammasome for the treatment of inflammatory diseases. *Nat Med* 2015;**21**:248–55. https://doi.org/10.1038/nm.3806
34. Bhende PM, Dickerson SJ, Sun X *et al.* X-box-binding protein 1 activates lytic Epstein–Barr virus gene expression in combination with protein kinase D. *J Virol* 2007;**81**:7363–70. https://doi.org/10.1128/JVI.00154-07
35. Shirley CM, Chen J, Shamay M *et al.* Bortezomib induction of C/EBPbeta mediates Epstein–Barr virus lytic activation in Burkitt lymphoma. *Blood* 2011;**117**:6297–303. https://doi.org/10.1182/blood-2011-01-332379
36. Guha P, Kaptan E, Gade P *et al.* Tunicamycin induced endoplasmic reticulum stress promotes apoptosis of prostate cancer cells by activating mTORC1. *Oncotarget* 2017;**8**:68191–207. https://doi.org/10.18632/oncotarget.19277
37. Cross BC, Bond PJ, Sadowski PG *et al.* The molecular basis for selective inhibition of unconventional mRNA splicing by an IRE1-binding small molecule. *Proc Natl Acad Sci USA* 2012;**109**:E869–878. https://doi.org/10.1073/pnas.1115623109
38. Papandreou I, Denko NC, Olson M *et al.* Identification of an Ire1alpha endonuclease specific inhibitor with cytotoxic activity against human multiple myeloma. *Blood* 2011;**117**:1311–4. https://doi.org/10.1182/blood-2010-08-303099
39. Ni H, Ou Z, Wang Y *et al.* XBP1 modulates endoplasmic reticulum and mitochondria crosstalk via regulating NLRP3 in renal ischemia/reperfusion injury. *Cell Death Discov* 2023;**9**:69. https://doi.org/10.1038/s41420-023-01360-x
40. Rohde C, Becker S, Krahling V. Marburg virus regulates the IRE1/XBP1-dependent unfolded protein response to ensure efficient viral replication. *Emerg Microbes Infect* 2019;**8**:1300–13. https://doi.org/10.1080/22221751.2019.1659552
41. Lerner AG, Upton JP, Praveen PV *et al.* IRE1alpha induces thioredoxin-interacting protein to activate the NLRP3 inflammasome and promote programmed cell death under irremediable ER stress. *Cell Metab* 2012;**16**:250–64. https://doi.org/10.1016/j.cmet.2012.07.007
42. Li X, Akinyemi IA, You JK *et al.* A mechanism-based targeted screen to identify Epstein–Barr virus-directed antiviral agents. *J Virol* 2020;**94**:e01179-20. https://doi.org/10.1128/JVI.01179-20
43. Li X, Burton EM, Bhaduri-McIntosh S. Chloroquine triggers Epstein–Barr virus replication through phosphorylation of KAP1/TRIM28 in Burkitt lymphoma cells. *PLoS Pathog* 2017;**13**:e1006249. https://doi.org/10.1371/journal.ppat.1006249
44. Li X, Kozlov SV, El-Guindy A *et al.* Retrograde regulation by the viral protein kinase epigenetically sustains the Epstein–Barr Virus latency-to-lytic switch to augment virus production. *J Virol* 2019;**93**:e00572–19. https://doi.org/10.1128/JVI.00572-19
45. Burton EM, Akinyemi IA, Frey TR *et al.* A heterochromatin inducing protein differentially recognizes self versus foreign genomes. *PLoS Pathog* 2021;**17**:e1009447. https://doi.org/10.1371/journal.ppat.1009447
46. Li H, Guan Y, Liang B *et al.* Therapeutic potential of MCC950, a specific inhibitor of NLRP3 inflammasome. *Eur J Pharmacol* 2022;**928**:175091. https://doi.org/10.1016/j.ejphar.2022.175091
47. Chen QL, Yin HR, He QY *et al.* Targeting the NLRP3 inflammasome as new therapeutic avenue for inflammatory bowel disease. *Biomed Pharmacother* 2021;**138**:111442. https://doi.org/10.1016/j.biopha.2021.111442
48. Sugiokto FG, Li R. Targeted eradication of EBV-positive cancer cells by CRISPR/dCas9-mediated EBV reactivation in combination with ganciclovir. *mBio* 2024;**15**:e0079524. https://doi.org/10.1128/mbio.00795-24
49. Wu M, Hau PM, Li L *et al.* Synthetic BZLF1-targeted transcriptional activator for efficient lytic induction therapy against EBV-associated epithelial cancers. *Nat Commun* 2024;**15**:3729. https://doi.org/10.1038/s41467-024-48031-8
50. Meng Q, Hagemeier SR, Fingeroth JD *et al.* The Epstein–Barr virus (EBV)-encoded protein kinase, EBV-PK, but not the thymidine kinase (EBV-TK), is required for ganciclovir and acyclovir inhibition of lytic viral production. *J Virol* 2010;**84**:4534–42. https://doi.org/10.1128/JVI.02487-09

Received: December 10, 2024. **Revised:** March 31, 2025. **Editorial Decision:** April 16, 2025. **Accepted:** April 25, 2025